Asian Journal of Chemistry; Vol. 36, No. 5 (2024), 1089-1092

ASIAN JOURNAL OF CHEMISTRY

https://doi.org/10.14233/ajchem.2024.31356

Antimicrobial Studies of Graphene Derivative Infused Polyaniline Nanocomposites

P.N. PRASEETHA[1,*], N.V. NISMA[2] and M.M. FEBA[1]

[1]Department of Chemical Engineering, Government Engineering College, Thrissur-680009, India
[2]Department of Chemistry, St. Mary's College, Thrissur-680020, India

*Corresponding author: E-mail: praseetha@gectcr.ac.in

Received: 5 February 2024; *Accepted*: 18 March 2024; *Published online*: 30 April 2024; AJC-21613

This study explores the synthesis and antimicrobial properties of graphene-based polyaniline (PANI) nanocomposites including pure PANI, PANI/graphene oxide (GO) and PANI/reduced graphene oxide (rGO). The composites were prepared using *in situ* and *ex situ* polymerization techniques. Characterization through X-ray diffraction (XRD) and Fourier transform infrared spectroscopy (FTIR) revealed the crystalline plane and prime characteristic peaks confirming nanocomposite formation. The antimicrobial properties were assessed using the Agar well-diffusion method against *Bacillus*, *Staphylococcus*, *Pseudomonas* and *Escherichia coli*. Pristine PANI exhibited higher bacterial inhibition zones compared to PANI/GO. Notably, PANI/rGO synthesized *ex situ* demonstrated superior antibacterial activity compared to *in situ* PANI/rGO composite.

Keywords: Polyaniline, Graphene oxide, Reduced graphene oxide, Polymerization, Antimicrobial activity.

INTRODUCTION

Graphene-based materials and their composites possess promising applications in a wide range of fields such as electronics, biomedical, membranes, flexible wearable sensors and actuators [1]. Potential applications are mainly driven by the progressive production of different graphene materials such as graphene oxide (GO), reduced graphene oxide (rGO), functionalized graphene oxide (fGO) and monolayer graphene, which is a single atom thick sheet of hexagonally arranged carbon atoms and can be used as a touch screen, nanoelectronics, *etc*. with particular focus on specific applications. GO has been popularly used as a nanofiller for fiber-reinforced polymer composites [2-4] and is reported to possess antimicrobial properties against various microbes. It can regain graphene like properties through additional reductive exfoliation treatments that convert GO to rGO. At this point, rGO becomes a good compromise between graphene and GO. Since, rGO has similar mechanical, optoelectronic or conductive properties to pristine graphene because it has a heterogeneous structure consisting of a graphene-like basal plane that is additionally decorated with structural defects and populated with regions containing oxidized chemical groups [5-7].

In the large field of nanotechnology, polymer matrix-based nanocomposites (PNCs) have become a prominent area of current research and development [8]. Several reviews have been published in the field of PNCs summarizing different aspects of PNCs with carbon nanomaterials as fillers [9-11]. However, due to its limited processing capability, stiffness and non-biodegradability, polyaniline (PANI) is limited in the biological applications. The main problem is its insufficient solubility, which is influenced by the inflexible backbone. Efforts to improve its processability have focused on chemical changes, notably doped PANI, composites form of PANI and other PANI derivatives. When compared to pure PANI, chemically changed PANI not only has greater processing capabilities but also has improved conductivity and anti-corrosion properties [12]. This combination successfully overcomes PANIs intrinsic disadvantages and thus improving the composite performance overall [13].

PANI and rGO composites have undergone extensive exploration for diverse applications, with a remarkable focus on thermoelectricity. Changing the concentration of rGO nanosheet composites has shown promise in enhancing the thermoelectric properties of PANI [14]. Beyond thermoelectricity, these composites serve as transparent counter electrodes in

dye sensitized solar cells, presenting an economical alternative to platinum [15]. The innovative hybrid composites, consisting of PANI columns applied to the surface of rGO, take advantage of the open-pore structure and excellent conductivity of the 3D rGO aerogel as well as the high capacitance contribution from the PANI [13].

This study focuses on the fabrication of different polymer matrix-based nanocomposites (PNCs) with PANI, the conducting polymer and organic semiconductors of the semi-flexible rod polymer family that can be synthesized by *in situ* polymerization of aniline monomer. Graphene-based material rGO is used as filler in these composites. PANI/GO composites were prepared by ultrasonication of GO in acidic medium by the *in situ* polymerization technique. The *in situ* polymerized PANI/GO was subsequently reduced using hydrazine hydrate as reducing agent inside the solution. This was achieved by adding an ammonia buffer solution resulting in the formation of a PANI/rGO composite. Later rGO was directly dispersed in the PANI to form the composite following the *ex situ* polymerization method. A comparative study of these composites based on their properties was performed and the antimicrobial activities of the composites were also studied.

EXPERIMENTAL

Synthesis of pure PANI and PANI/reduced graphene oxide nanocomposites: The monomer aniline (Merck Life Science Pvt. Ltd., Mumbai, India) and oxidizing agent ammonium persulfate (APS) (Merck Life Science Pvt. Ltd., Mumbai, India), in the acidic medium (HCl) (Nice Chemicals Pvt. Ltd, Cochin, India) are used for the chemical polymerization. Reduced graphene oxide (rGO) (dia.: 0.8-2.0 nm) (Shilpent Enterprises, India), graphene oxide (GO) (dia.: 0.8-2.0 nm) (Shilpent Enterprises, India) were used as the fillers and the reducing agent hydrazine hydrate (Spectrum Chemicals Pvt. Ltd.), ammonium buffer solution (Nice Chemicals Pvt. Ltd, Cochin) were used for the synthesis of PANI/rGO by *in situ* polymerization. The solvent acetone was used for the solution casting in *ex situ* polymerization of PANI/rGO.

Polymerization of aniline: In 5 mL aniline, 100 mL of 1 M HCl was added into a 500 mL beaker with constant stirring using magnetic stirrer followed by the addition of 100 mL of 1 M ammonium persulfate solution dropwise. The temperature was maintained below 5 ºC by placing it in an ice bath. It was then kept on the magnetic stirrer for 24 h to complete the reaction. The green emeraldine salt form of PANI is formed and washed with 0.1M HCl, followed by washing with deionized water, acetone and finally dried in an oven at 60 ºC.

Synthesis of PANI/rGO nanocomposite by *in situ* polymerization: Different compositions of graphene oxide (GO) (1%, 2%, 3% and 4% wt.) in an acidic medium (100 mL of 1 M HCl) were ultrasonicated with 5 mL aniline for 1 h using magnetic stirring. Then, 100 mL of ammonium persulphate (1 M) was added dropwise with constant stirring for 24 h by maintaining the temperature below 5 ºC. The GO/PANI nanocomposites formed were washed with 1 M HCl followed by distilled water until the filtrate becomes colourless. It's pH was adjusted to 10 by neutralizing with ammonia buffer solution. Subsequently, 2 mL of hydrazine hydrate was introduced into 75 mL aqueous solution containing PANI/GO composite at 95 ºC for 1 h. During this process, the reduction of GO to rGO occurred, resulting in the production of a PANI/rGO nanocomposite, which was dried in an oven at 60 ºC.

Synthesis of PANI/rGO nanocomposite by *ex situ* polymerization: The polymeric nanocomposite was prepared by solvent casting method. A 1 g of PANI was mixed with 20 mL of acetone followed by the addition of different weight percentages (0.5%, 1%, 1.5%, 2%) of rGO and stirred for 2 h. The PANI/rGO nanocomposite was washed with distilled water to remove the unreacted PANI and then the residue was dried at 60 ºC.

Characterization: The infrared spectrum was recorded using Perkin-Elmer spectrum two, Model L160000A, wavelength range 8300-350 cm^{-1} optimized using KBr beam splitter. The powder XRD patterns for the samples were obtained by using the X-ray diffraction (XRD) system (PANALYTICAL) and Aeris Research with Cu$K\alpha$ radiation (λ = 0.1540598 nm) in the Bragg angle range of 10-90º through scan access goniometer.

Antibacterial study: Antimicrobial activity was determined by the Agar well-diffusion method according to the National committee for Clinical Laboratory Standards (NCCLS) [16]. The agar plates were inoculated with a standardized inoculum of the test microorganism. Then the wells (about 8 mm in diameter) were punched and the test compound at a desired concentration was added into the wells and allowed to diffuse at room temperature for 2 h and the wells containing the same volume of DMSO served as negative controls. The Petri dishes were incubated at 37 ºC for 48 h. After incubation, the diameters of the inhibition growth zones were measured. Inoculums containing bacterial culture (using two Gram-positive (*Bacillus*, *Staphylococcus*) and two Gram-negative bacteria (*Pseudomonas and Escherichia coli*) were spread on nutrient agar plates with a sterile swab moistened with the bacterial suspension.

RESULTS AND DISCUSSION

FTIR studies: FTIR analysis of PANI, PANI/GO, PANI/rGO composites were conducted and the corresponding spectra are shown in Fig. 1. The main characteristic peaks of PANI appeared at 3436, 2998, 1554, 1442, 1288 cm^{-1}. Based on the peak of 3448 cm^{-1}, it can be seen that the intensity of the peak increases with an increasing composition of GO. This is due to the hydrogen bond formed between the possible oxygen-containing group of GO and the NH group of PANI. The presence of both peaks GO and PANI confirmed the formation of the PANI/GO nanocomposites [17-19]. In the PANI/rGO nanocomposites, the absorption peaks at 3462, 1556 and 1484 cm^{-1} should be assigned to the stretching vibration of -N-H group, quinoid ring (-N=Q=N-) and benzenoid ring (N-B-N), respectively [20].

XRD studies: Fig. 2 shows the XRD spectrum of pure PANI and PANI/GO nanocomposite at room temperature. PANI shows the main diffraction peaks at 8.54º, 14.93º, 15.71º, 21.53º and 26.32º. The PANI shows one sharp peak centered around

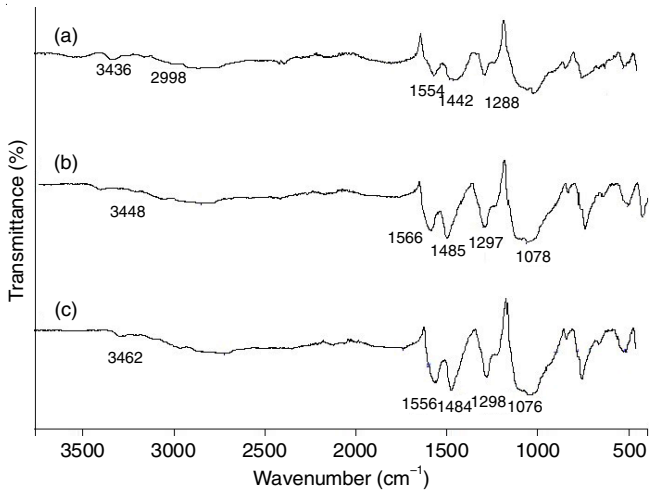

Fig. 1. FTIR spectra of polymer composites (a) pure PANI, (b) PANI/GO and (c) PANI/rGO

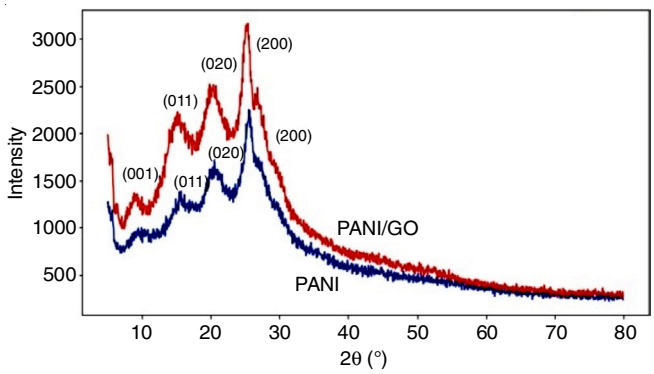

Fig. 2. XRD spectrum of pure PANI and PANI/GO nanocomposite

26.30 with other two low intensity peaks with their position around 21.53º and 15.71º, corresponding to (200), (020) and (011) semi-crystalline planes of PANI in its emeraldine salt form [21]. The polymer is inherently semi-crystalline, as the pattern has sharp peaks due to the presence of benzene-like and quinone-like groups in the PANI. The interplanar crystallinity and crystal size were calculated using Bragg's law and the Debye-Scherer equation (eqn. 1):

$$\frac{K\lambda}{\beta\cos\theta} \quad (1)$$

where K is the dimensionless form factor (0.9), full width and half maximum. From the XRD patterns, the crystal size was found to be 2.10 nm.

The XRD patterns of the synthesized PANI/GO nanocomposites are similar to those of PANI indicating that the molecular chain structure of PANI was not wrecked. No obvious peak of GO was observed in the XRD pattern of PANI/GO, indicating that GO exhibited almost no agglomeration but dispersed completely with the polymerized substrate during the synthesize of PANI/GO nanocomposites [22-24].

The XRD patterns of PANI/rGO nanocomposites by both *in situ* and *ex situ* methods are shown in Fig. 3. Herein, it is observed that PANI/rGO *ex situ* nanocomposite exhibit the peak at 21.5º and 26.3º corresponding to (020) and (200) reflections, respectively from the crystalline planes of PANI. The appearance of peaks at 21.5º and 26.3º in PANI/rGO *ex situ* nanocomposites provides evidence that the unit structure of PANI chains remains intact even after the composite is formed with rGO. However, the PANI/rGO *in situ* nanocomposite exhibits significant differences in the relative intensity of the peak features of PANI, indicating that the reducing agent affects the crystalline nature of PANI. Furthermore, it is evident that the use of hydrazine hydrate in the reduction of PANI/GO has a significant impact on the crystallinity of PANI [25].

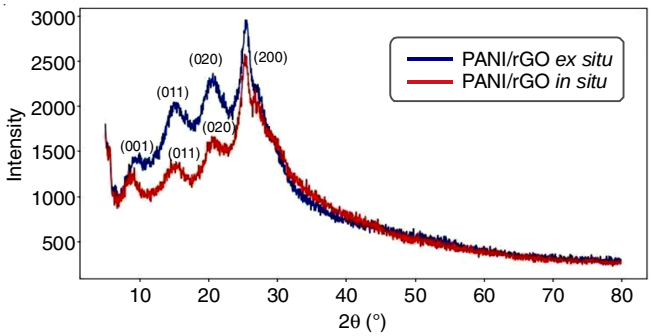

Fig. 3. XRD spectrum of PANI/rGO nanocomposite by *in situ* and *ex situ* polymerization

Antibacterial studies: The PANI, PANI/GO, PANI/rGO *in situ* and PANI/rGO *ex situ* were tested against Gram-positive bacteria (*Bacillus* and *Staphylococcus*) and Gram-negative bacteria (*Pseudomonas* and *E. coli*). The experiment shows that the activity of all four bacteria was affected by PANI. It was found that PANI/GO was active against the Gram-positive bacteria *Bacillus* and *Staphylococcus* and at higher concentrations against *E. coli* (Gram -ve). At higher concentrations of PANI/rGO *ex situ*, a zone of inhibition was observed in Gram-positive bacteria (*Bacillus* and *Staphylococci*) indicating the antimicrobial activity of the nanocomposite.

Results (Fig. 4) showed that PANI/rGO *in situ* nanocomposites show no antibacterial activity, which suggests that in PANI/rGO *ex situ* nanocomposites contain higher PANI content in the *ex situ* method. The hierarchy of antibacterial effectiveness among the composites is as follows: PANI > PANI/GO > PANI/rGO *ex situ* > PANI/rGO *in situ*.

Conclusion

In this work, the antibacterial characteristics of pure polyaniline (PANI), PANI/graphene oxide (GO) and PANI/reduced graphene oxide (rGO) nanocomposites are investigated in this study, along with their methods of synthesis. The PANI/GO nanocomposite was prepared by *in situ* chemical oxidative polymerization, whereas PANI/rGO by both *in situ* and *ex situ* polymerization. All the materials were well characterized by XRD analysis and FTIR spectroscopy. The X-ray diffraction patterns of PANI show the size of nanoscale particles and no peak of GO was observed in the XRD pattern of PANI/GO. The XRD patterns of PANI/rGO *in situ* indicates a loss of crystallinity of PANI, which is associated with the simultaneous reduction of GO, while the crystalline structure of PANI in *ex situ* PANI/rGO was preserved. The antimicrobial studies were performed using the agar well diffusion technique using Gram-

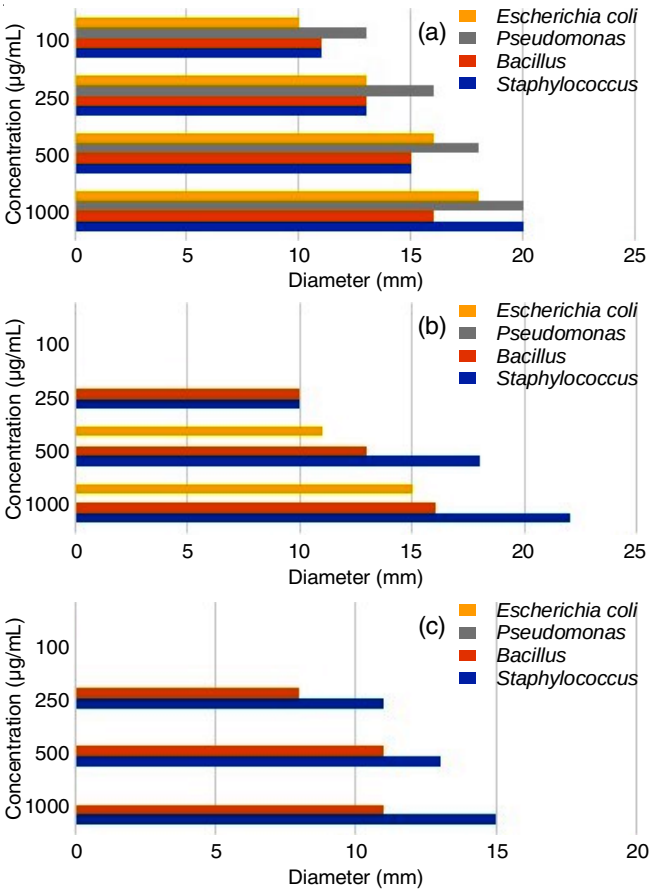

Fig. 4. Antimicrobial activity of (a) pure PANI, (b) PANI/GO, (c) PANI/rGO nanocomposite prepared by *ex situ* method

positive and Gram-negative bacteria. It was found that PANI/GO composite has antibacterial activity against *Bacillus, Staphylococcus* and *Escherichia coli*. On the other hand, PANI/rGO *ex situ* nanocomposite exhibit zones of inhibition against Gram-positive bacteria, which means that PANI/rGO *ex situ* composites show more activity than PANI/rGO *in situ* nanocomposites, *i.e.* PANI/rGO *ex situ* has more PANI nature than the *in situ* method.

CONFLICT OF INTEREST

The authors declare that there is no conflict of interests regarding the publication of this article.

REFERENCES

1. V.B. Mohan, K.-T. Lau, D. Hui and D. Bhattacharyya, *Composites B Eng.*, **142**, 200 (2018); https://doi.org/10.1016/j.compositesb.2018.01.013
2. Y. Zhu, S. Murali, W. Cai, X. Li, J. Suk, J. Potts and R. Ruoff, *Adv. Mater.*, **22**, 3906 (2010); https://doi.org/10.1002/adma.201001068
3. X. Fu, J. Lin, Z. Liang, R. Yao, W. Wu, Z. Fang, W. Zou, Z. Wu, H. Ning and J. Peng, *Surf. Interfaces*, **37**, 102747 (2023); https://doi.org/10.1016/j.surfin.2023.102747
4. L. Sun and B. Fugetsu, *Mater. Lett.*, **109**, 207 (2013); https://doi.org/10.1016/j.matlet.2013.07.072
5. R. Tarcan, O. Todor-Boer, I. Petrovai, C. Leordean, S. Astilean and I. Botiz, *J. Mater. Chem. C Mater. Opt. Electron. Devices*, **8**, 1198 (2020); https://doi.org/10.1039/C9TC04916A
6. D.Y. Gui, C.L. Liu, F.Y. Chen and J.H. Liu, *Appl. Surf. Sci.*, **307**, 172 (2014); https://doi.org/10.1016/j.apsusc.2014.04.007
7. C. Chen, J. Xi, E. Zhou, L. Peng, Z. Chen and C. Gao, *Nano-Micro Lett.*, **10**, 26 (2018); https://doi.org/10.1007/s40820-017-0179-8
8. D.R. Paul and L.M. Robeson, *Polymer*, **49**, 3187 (2008); https://doi.org/10.1016/j.polymer.2008.04.017
9. J. Potts, D. Dreyer, C. Bielawski and S. Ruoff, *Polymer*, **52**, 5 (2011); https://doi.org/10.1016/j.polymer.2010.11.042
10. G. Ciric-Marjanovic, *Synth. Met.*, **170**, 31 (2013); https://doi.org/10.1016/j.synthmet.2013.02.028
11. C. Moreno, M. Vilas-Varela, B. Kretz, A. Garcia-Lekue, M.V. Costache, M. Paradinas, M. Panighel, G. Ceballos, S.O. Valenzuela, D. Peña and A. Mugarza, *Science*, **360**, 199 (2018); https://doi.org/10.1126/science.aar2009
12. G. Liao, Q. Li and Z. Xu, *Progr. Org. Coat.*, **126**, 35 (2019); https://doi.org/10.1016/j.porgcoat.2018.10.018
13. S. Yasami, S. Mazinani and M.S. Abdouss, *J. Energy Storage*, **72**, 108807 (2023); https://doi.org/10.1016/j.est.2023.108807
14. D. Ebrahimibagha, S.A. Armida, S. Datta and M. Ray, *Comput. Mater. Sci.*, **232**, 112601 (2024); https://doi.org/10.1016/j.commatsci.2023.112601
15. S.V. Kuppu, M. Senthilkumaran, V. Sethuraman, C. Saravanan, M. Balaji, N. Ahmed, S. Mohandoss, Y.R. Lee, J. Anandharaj and T. Stalin, *J. Phys. Chem. Solids*, **173**, 111121 (2023); https://doi.org/10.1016/j.jpcs.2022.111121
16. National Committee for Clinical Laboratory Standards, Performance Standards for Antimicrobial Disk Susceptibility Tests, National Committee for Clinical Laboratory Standards, Approved Standard M2-A6. Wayne, PA: USA (1997).
17. V. Shalini, M. Navaneethan, S. Harish, J. Archana, S. Ponnusamy, H. Ikeda and Y. Hayakawa, *Appl. Surf. Sci.*, **493**, 1350 (2019); https://doi.org/10.1016/j.apsusc.2019.06.249
18. U.R. Farooqui, A.L. Ahmad and N.A. Hamid, *Renew. Sustain. Energy Rev.*, **82**, 714 (2018); https://doi.org/10.1016/j.rser.2017.09.081
19. W. Wang, J. Yan, J. Liu, D. Ou, Q. Qin, B. Lan, Y. Ning, D. Zhou and Y. Wu, *Electrochim. Acta*, **282**, 835 (2018); https://doi.org/10.1016/j.electacta.2018.06.121
20. J.E. Abraham, A.K. Das, M. Pandey and M. Balachandran, *Polym. Bull.*, **77**, 4023 (2020); https://doi.org/10.1007/s00289-019-02954-1
21. Y. Zhang, J. Liu, Y. Zhang, J. Liu and Y. Duan, *RSC Adv.*, **7**, 54031 (2017); https://doi.org/10.1039/C7RA08794B
22. H.L. Wang, Q.L. Hao, X.J. Yang, L.D. Lu and X. Wang, *ACS Appl. Mater. Interfaces*, **2**, 821 (2010); https://doi.org/10.1021/am900815k
23. R. Gupta, Z. Alahmed and F. Yakuphanoglu, *Mater. Lett.*, **112**, 75 (2013); https://doi.org/10.1016/j.matlet.2013.09.011
24. D.R. Dreyer, S. Park, C.V. Bielawski and R.S. Ruoff, *Chem. Soc. Rev.*, **39**, 228 (2010); https://doi.org/10.1039/B917103G
25. T. Bautkinová, A. Sifton, E.M. Kutorglo, M. Dendisová, D. Kopecký, P. Ulbrich, P. Mazúr, A. Laachachi and F. Hassouna, *Colloids Surf. A Physicochem. Eng. Asp.*, **589**, 124415 (2020); https://doi.org/10.1016/j.colsurfa.2020.124415